

## Visible photoluminescence from oxidized Si nanometer-sized spheres: Exciton confinement on a spherical shell

Yoshihiko Kanemitsu

*Institute of Physics, University of Tsukuba, Tsukuba, Ibaraki 305, Japan*

Tetsuo Ogawa, Kenji Shiraishi, and Kyozauro Takeda

*NTT Basic Research Laboratories, Musashino, Tokyo 180, Japan*

(Received 22 February 1993; revised manuscript received 17 May 1993)

We report strong visible photoluminescence (PL) at room temperature from oxidized Si nanometer-sized spheres with a spherical crystalline Si (*c*-Si) core and an amorphous SiO<sub>2</sub> (*a*-SiO<sub>2</sub>) surface layer. The peak energy of the broad PL spectrum is about 1.65 eV, which is independent of the core diameter. We propose a model in which excitons are confined on a spherical shell, an interfacial layer between the *c*-Si core and the *a*-SiO<sub>2</sub> surface layer, and in which the exciton confinement enhances the oscillator strength and the PL intensity.

Recently, many attempts have been made to produce quasi-direct-gap semiconductor nanostructures from indirect-gap materials, especially Si (Ref. 1) and Ge (Ref. 2) nanocrystallites, which exhibit strong visible photoluminescence (PL) even at room temperature. Many researchers are trying to clarify the origin of the strong visible PL experimentally and theoretically. Recent models are based on either quantum-confinement effects<sup>1,3-6</sup> or localized states at the surface of nanocrystallites.<sup>7</sup> However, the mechanism of this PL still remains unclear. This is partly because the structure and the composition of nanocrystalline samples are difficult to control and thus difficult to know with certainty. We therefore experimented with oxidized Si nanometer-sized spheres that were prepared in a controlled manner and known to consist of a spherical crystalline Si (*c*-Si) core and an amorphous SiO<sub>2</sub> (*a*-SiO<sub>2</sub>) surface layer.

The surface of luminescent Si nanocrystallites is usually terminated by hydrogen or oxygen atoms,<sup>7,8</sup> which cause the electronic properties of the near-surface region to differ from those of the *c*-Si core. In this sense, the surface can also serve as a low-dimensional system inducing quantum confinements. To distinguish the quantum-confinement effects in a surface region from the usual confinement in a core, we need to know the size dependence of the PL properties of the nanocrystallites *with an identical surface chemical structure*. Oxidized Si nanometer-sized spheres are good samples, because it is possible to control the size of the *c*-Si core.

In this paper, we report experimental results of the PL properties of oxidized Si nanometer-sized spheres whose surfaces are passivated by an *a*-SiO<sub>2</sub> layer. Analysis of these results leads us to propose a model in which these oxidized Si nanometer-sized spheres consist of three regions, and excitons are confined in a middle, spherical shell region (an interfacial layer between the *c*-Si core and the *a*-SiO<sub>2</sub> surface layer). According to this model, the oscillator strength is enhanced due to the low-dimensional exciton nature in the shell region.

The Si nanometer-sized spheres were produced by laser breakdown of silane (SiH<sub>4</sub>) gas.<sup>9</sup> Pure SiH<sub>4</sub> gas was in-

troduced into the vacuum chamber (background pressure < 10<sup>-6</sup> Torr) and the pressure of the SiH<sub>4</sub> gas was held at 10 (sample 1), 15 (sample 2), or 20 (sample 3) Torr. The average diameter of the Si nanometer-sized spheres was controlled by this pressure. Laser pulses (~200 mJ per pulse at 1.06 μm, 10 ns pulse duration) from a Nd<sup>3+</sup>:YAG (where YAG denotes yttrium aluminum garnet) laser system were focused, and a spark was observed at the focal point. The Si nanometer-sized spheres were deposited on quartz or Ge wafer substrates.<sup>10</sup> In as-grown samples, we observed no PL at room temperature. The samples oxidized at room temperature in a clear-air box exhibited strong visible PL at room temperature. Several samples with different core diameters and identical surface chemical structures were prepared and their PL spectra were measured using ~50-mW cm<sup>-2</sup>, 325-nm excitation light from a He-Cd laser. The spectral sensitivity of the measuring system was calibrated by using a tungsten standard lamp. The temperature was varied from 10 to 300 K by controlling the flow rate of cold He gas in a cryostat.

Crystallinity and size of the oxidized Si nanometer-sized spheres were studied by high-resolution transmission electron microscopy (TEM) using a JELO 2010 system operated at 200 keV. A typical TEM image of the oxidized Si nanometer-sized spheres is shown in Fig. 1(a). The interplane spacing of the TEM images of the Si core is consistent with the (111) planes of the diamond structure. Sharp rings in the electron-diffraction pattern also indicated that the core is *c*-Si with the diamond structure. This *c*-Si core is surrounded by an ~1.6-nm-thick layer of what Fourier-transform infrared spectroscopy indicated is amorphous silicon oxide (a peak near 1100 cm<sup>-1</sup> due to the Si-O-Si asymmetric stretching mode was observed). To confirm the composition of this surface layer, we analyzed the oxidized nanometer-sized spheres by x-ray photoemission spectroscopy (XPS) at a base pressure of 2 × 10<sup>-8</sup> Torr, using a Perkin-Elmer 5500 system. A detailed scan of the silicon 2*p* region in oxidized Si nanometer-sized spheres on a Ge wafer substrate is shown in Fig. 1(b). The XPS data show that an *a*-SiO<sub>2</sub>

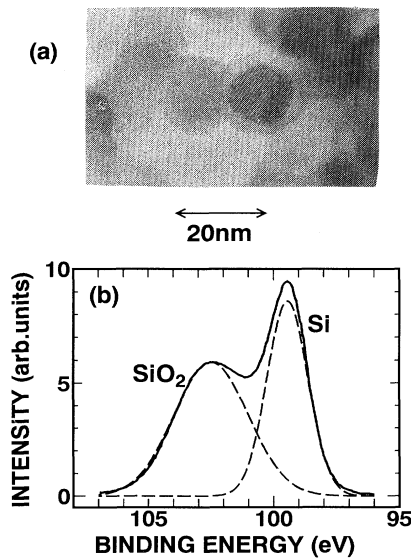


FIG. 1. (a) High-resolution TEM lattice image of oxidized Si nanometer-sized spheres composed of a *c*-Si core and an  $\sim 1.6$ -nm-thick *a*-SiO<sub>2</sub> surface layer. (b) XPS spectrum of the silicon 2*p* region from the oxidized Si nanometer-sized spheres.

layer is formed on the surface of the Si sphere. These TEM and XPS examinations clearly indicate that the oxidized Si nanometer-sized spheres consist of a *c*-Si core and a 1.6-nm-thick *a*-SiO<sub>2</sub> surface layer.

The size distributions of oxidized Si nanometer-sized-sphere samples are shown in Fig. 2. The distribution of the overall diameter of these nanometer-sized spheres can be described by a log-normal function.<sup>11</sup> This overall diameter  $D_{\text{total}}$  includes the diameter of the *c*-Si core  $D_{\text{core}}$  and the 1.6-nm thickness of the SiO<sub>2</sub> surface layer:  $D_{\text{total}} = D_{\text{core}} + 3.2$  nm. The average diameter  $\langle D_{\text{total}} \rangle$  and the standard deviation  $\sigma$  are tabulated in Table I.

PL spectra from the three samples of oxidized Si nanometer-sized spheres are plotted in Fig. 3(a). All the spectra are broad and have a peak around 1.65 eV. That is, the PL peak energy is independent of the average diameter of the *c*-Si core. On the other hand, the PL intensity increases with the number of the oxidized Si nanometer-sized spheres that have a small  $D_{\text{core}}$ : The PL

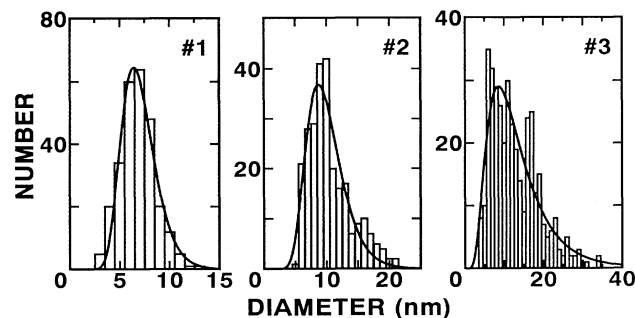


FIG. 2. The size distribution of oxidized Si nanometer-sized spheres. The solid curves are optimum log-normal functions.

TABLE I. Sample parameters including the average diameter  $\langle D_{\text{total}} \rangle$ , the standard deviation  $\sigma$ , the PL peak energy  $E_{\text{PL}}$ , the PL intensity  $I_{\text{PL}}$ , and the fraction of oxidized Si nanometer-sized spheres with  $D_{\text{core}} \leq 9$  nm,  $V_9^a$ .

Sample No.	$\langle D_{\text{total}} \rangle$ (nm)	$\sigma$ (nm)	$E_{\text{PL}}$ (eV)	$I_{\text{PL}}^a$	$V_9^a$
1	7.0	1.8	1.65	100	100
2	10.0	3.1	1.65	58	52
3	13.3	7.7	1.65	11	10

<sup>a</sup>Normalized values.

intensity is approximately proportional to the volume fraction  $V_9$  of the oxidized Si nanometer-sized spheres of  $D_{\text{core}} \leq \sim 9$  nm, indicating that these smaller nanometer-sized spheres contribute to the strong PL.

As shown in Fig. 3(b), the temperature dependence of the PL intensity  $I_{\text{PL}}$  is unusual. The PL intensity increases with rising temperature up to  $\sim 150$  K, and then decreases very gradually. At temperatures above 150 K, the nonradiative recombination rate increases and the PL intensity decreases. On the other hand, there is a linear relationship in the  $\log I_{\text{PL}} - 1/T$  plot (the Arrhenius plot) at  $T < \sim 150$  K and the slope gives an activation energy of  $\sim 5$  meV. This unusual temperature dependence of the PL intensity cannot be fully explained by the usual quantum-confinement models<sup>1,3-6</sup> because, according to these models, nonradiative recombination processes become dominant with increasing temperature and the PL intensity decreases. This temperature dependence at  $T < 150$  K will be discussed later in this paper.

To evaluate the possible origins of the strong PL at 1.65 eV, we recall that strong PL is observed only when the Si core is covered by an *a*-SiO<sub>2</sub> layer and first consider the electronic and optical properties of the *c*-Si core and the *a*-SiO<sub>2</sub> surface layer.

(a) *The c-Si core.* For core sizes of nanometer order, the band-gap energy depends sensitively on the core size.

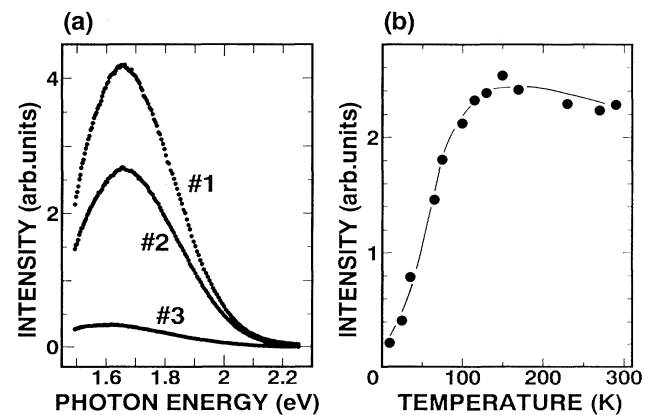


FIG. 3. (a) Photoluminescence spectra under 325-nm excitation for three samples at room temperature. (b) Temperature dependence of the PL intensity of sample 1. Similar temperature dependence was observed in samples 2 and 3. The solid curve is a guide to the eye.

According to an effective-mass theory,<sup>6</sup> the lowest ( $1s$ ) exciton energy of the  $c$ -Si core changes from 1.3 eV for 10 nm diameter to 2.0 eV for 4 nm diameter. This is inconsistent with the size-independent PL peak energy. Moreover, the electronic properties of a  $c$ -Si core more than several nanometers in diameter are thought to be similar to those of *bulk* Si.<sup>6,12</sup> Therefore, the indirect-to-direct transition in the band gap may not occur in our samples. The optical transition strength would then be small because of the indirect character, and this would result in no strong PL.

(b) *The  $a$ -SiO<sub>2</sub> surface.* Although  $a$ -SiO<sub>2</sub> has a direct band gap, this surface layer does not itself contribute to the visible PL because the band-gap energy is out of the visible range ( $> 8$  eV). However, this layer plays the following roles: (i) the reduction of the number of surface dangling bonds that act as nonradiative recombination centers of the  $c$ -Si core, (ii) the quantum confinement of photogenerated carriers within the  $c$ -Si core due to the large band gap of  $a$ -SiO<sub>2</sub>, and (iii) the creation of a novel electronic state in an interfacial region (this state is due to oxygen atoms interconnecting the  $c$ -Si core with the  $a$ -SiO<sub>2</sub> surface layer).

Because the size-independent PL peak energy and the unusual temperature dependence of the PL intensity imply that visible PL processes have an origin other than the quantum confinements in the  $c$ -Si core, we stress the importance of the interfacial region between the  $c$ -Si core and the  $a$ -SiO<sub>2</sub> surface layer. We also propose a three-region model for oxidized Si nanometer-sized spheres of (a) a  $c$ -Si core with diameter  $D_{\text{core}}$ , (b) an  $a$ -SiO<sub>2</sub> surface layer with a finite thickness (1.6 nm), and (c) an interfacial layer between (a) and (b). In this model, the interfacial region plays the most important role in the PL process.

(c) *The interfacial region.* The composition ratio of a silicon-oxygen compound in this region should be intermediate between that of  $a$ -SiO<sub>2</sub> (Si:O = 1:2) and that of  $c$ -Si (Si:O = 1:0). That is, this region contains nonstoichiometric amounts of oxygen atoms. In an incompletely oxidized Si layer, oxygen atoms play important roles in electronic structures. *Ab initio* calculations<sup>13,14</sup> indicate that oxygen atoms may reduce the band-gap energy to be smaller than that of the  $c$ -Si core. Photogenerated electrons, holes, and excitons are then confined in this thin interfacial region.

To understand the most essential feature of the electronic properties of this thin region, we use the result of the *ab initio* calculations for the one-sided planar siloxene compound,<sup>14–16</sup> because this compound has an intermediate composition ratio (Si:O) and a thin layer structure. The most characteristic feature is that, in striking contrast to the planar Si sheet<sup>17</sup> and the bulk Si crystal, this layer has a *direct* band gap of 1.7 eV at the  $\Gamma$  point. A schematic diagram of the band-gap energy is drawn in Fig. 4. The gap energy in the interfacial region is about 1.7 eV independent of  $D_{\text{core}}$ , while the gap energy in the  $c$ -Si core region depends on  $D_{\text{core}}$ .

We exploit here the exciton properties of the interfacial layer. The low-dimensional excitonic effects critically affect the optical properties of the nanometer-sized struc-

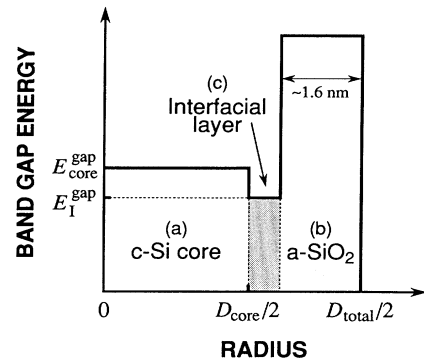


FIG. 4. Energy-gap diagram of the three-region model. The band-gap energy of the interfacial layer  $E_I^{\text{gap}}$  is  $\sim 1.6$  eV, including the exciton binding energy. The energy gap of the  $c$ -Si core  $E_{\text{core}}^{\text{gap}}$  increases with decreasing core diameter. In the case of  $D_{\text{core}} \leq 5\text{--}7$  nm, the exciton is confined in (c) the interfacial region, surrounded by (a) the  $c$ -Si core and (b) the  $a$ -SiO<sub>2</sub> surface layer.

tures.<sup>3</sup> When the band-gap energy of the interfacial layer is lower than that of the  $c$ -Si core, the exciton is subject to a confinement potential and is confined on the interfacial spherical-shell region. The condition for exciton confinement is roughly determined by the relative magnitude of the band-gap energy of each region. The  $a$ -SiO<sub>2</sub> surface region forms a high-potential barrier to confine the exciton inside. Theoretical calculations<sup>6</sup> indicate that the energy gap of the  $c$ -Si core of  $D_{\text{core}} \leq 5\text{--}7$  nm is higher than that of the interfacial layer. As a result, when  $D_{\text{core}} \leq 5\text{--}7$  nm, the exciton is confined in the interfacial shell region (see Fig. 4). We explicitly evaluate the properties of the exciton confined in this shell by using an effective-mass approximation. The two-dimensional exciton<sup>18,19</sup> is assumed and the reduced masses are calculated from the results of the *ab initio* calculation.<sup>14</sup> When the polarization direction is parallel to the interfacial layer, the two-dimensional exciton confinement increases the oscillator strength to about 15 times what it would be in absence of the exciton effects,<sup>16</sup> or four orders of magnitude greater than the oscillator strength in a  $c$ -Si core with  $D_{\text{core}} \leq 5\text{--}7$  nm.<sup>6,16</sup> Therefore, the exciton confinement in the interfacial layer is a possible origin of the strong 1.65-eV PL from oxidized Si nanometer-sized spheres.

Let us now consider the localized exciton as an origin of the size-independent PL of Si nanometer-sized spheres. If the visible PL is caused by the radiative recombination of localized excitons at defects or disorders in the  $c$ -Si core, the PL peak energy from localized states is less than the band-gap energy of the  $c$ -Si core [2.0 eV for  $D_{\text{core}} = 4$  nm (Ref. 6)] and the size dependence of the PL spectrum is very weak. However, the localized states usually act as *nonradiative centers*. In fact, we can observe the visible PL after the surface defect states are passivated by  $a$ -SiO<sub>2</sub>. Moreover, in the localized exciton model, there is no answer as to why the PL energy peak is 1.65 eV and why the PL is very strong even at room temperature. At present, we emphasize that the strong 1.65-eV PL is

caused by the exciton confinement in the interfacial region rather than by localized excitons at defects or disorders in the *c*-Si core.

We also consider the usual temperature dependence of the PL intensity. According to our three-region model, a process of the radiative recombination proceeds as follows: The photogeneration of excitons mainly occurs within the *c*-Si core. Some of the excitons in the core transfer to the interfacial layer by a thermally activated diffusion process. The strong PL is then caused by the radiative recombination of excitons confined in the interfacial layer. In this scenario, the diffusive transfer of excitons from the core to the interfacial layer increases with increasing temperature, resulting in the unusual temperature dependence of the PL intensity shown in Fig. 3(b). This exciton-transfer picture also explains why the PL intensity depends on the size of the *c*-Si core, while the PL peak energy is independent of core size: The smaller the core is, the more the efficiency of exciton transfer from the core to the interfacial layer is increased. The experimental results show that only the oxidized Si nanometer-sized spheres with  $D_{\text{core}} \leq 9$  nm contribute to the strong PL at 1.65 eV, and the theoretical evaluation of  $D_{\text{core}}$  (5–7 nm) agrees roughly with this finding.

The characteristic features of observed strong visible PL (the size-independent 1.65-eV PL, the size-dependent

PL intensity, and the curious temperature dependence of the PL intensity) are explained by the three-region model. For the size of our nanometer-sized-sphere samples, the exciton-confinement effect in the *c*-Si core is of little importance. We again stress that our argument relies on the exciton-confinement effect. If we ignore either the excitonic or the confinement effects, we would expect no strong PL.

In conclusion, we have prepared oxidized Si nanometer-sized spheres and have observed strong PL from them. We conclude that the interfacial Si layer between the *c*-Si core and the *a*-SiO<sub>2</sub> surface layer plays an important role in the PL process. We presented a three-region model that explains the size-independent 1.65-eV PL and the unusual temperature dependence of the PL intensity. The strong PL is caused by the radiative recombination of low-dimensional excitons confined in the interfacial layer. Even if this novel PL mechanism applies only to oxidized Si nanometer-sized spheres, our analysis is one step toward an understanding of the physics of the optical properties of Si nanostructures.

The authors thank H. Uto, Y. Masumoto, and T. Takagahara for discussions and T. Kawaguchi for providing the samples.

- 
- <sup>1</sup>L. T. Canham, *Appl. Phys. Lett.* **57**, 1046 (1990); A. G. Cullis and L. T. Canham, *Nature* **353**, 335 (1991).
- <sup>2</sup>Y. Kanemitsu *et al.*, *Appl. Phys. Lett.* **61**, 2187 (1992).
- <sup>3</sup>T. Ohno, K. Shiraishi, and T. Ogawa, *Phys. Rev. Lett.* **69**, 2400 (1992).
- <sup>4</sup>A. J. Read *et al.*, *Phys. Rev. Lett.* **69**, 1232 (1992); F. Buda, J. Kohanoff, and M. Parinello, *ibid.* **69**, 1272 (1992).
- <sup>5</sup>R. Tsu *et al.*, *Appl. Phys. Lett.* **60**, 112 (1992); M. W. Cole *et al.*, *ibid.* **60**, 2800 (1992).
- <sup>6</sup>T. Takagahara and K. Takeda, *Phys. Rev. B* **46**, 15 578 (1992).
- <sup>7</sup>M. A. Tischler *et al.*, *Appl. Phys. Lett.* **60**, 639 (1992); J. C. Tsang *et al.*, *ibid.* **60**, 2279 (1992); C. Tai *et al.*, *ibid.* **60**, 1700 (1992); V. Petrovan-Koch *et al.*, *ibid.* **61**, 943 (1992); J. C. Vial *et al.*, *Phys. Rev. B* **45**, 14 171 (1992).
- <sup>8</sup>T. Matsumoto, T. Futagi, H. Mimura, and Y. Kanemitsu, *Phys. Rev. B* **47**, 13 876 (1993).
- <sup>9</sup>W. R. Cannon *et al.*, *J. Am. Ceram. Soc.* **65**, 324 (1982); T. Kawaguchi and S. Miyashima, *Bull. Am. Phys. Soc.* **37**, 719 (1992).
- <sup>10</sup>Semiconductor nanocrystallites are usually dispersed in matrices such as glasses, polymers, and crystals. However, in our samples, Si nanometer-sized spheres are not in matrices. Moreover, the shape of our Si crystallite is spherical.
- <sup>11</sup>A. M. Law and W. D. Kelton, *Simulation Modeling and Analysis* (McGraw-Hill, New York, 1986), p. 164.
- <sup>12</sup>Y. Kayanuma, *Oyo Buturi* **61**, 796 (1992) [in Japanese].
- <sup>13</sup>P. Deak *et al.*, *Phys. Rev. Lett.* **69**, 2531 (1992).
- <sup>14</sup>K. Takeda and K. Shiraishi, *Solid State Commun.* **85**, 301 (1993).
- <sup>15</sup>Incomplete oxygen termination on the Si sheet has also been discussed in Ref. 16. A more detailed evaluation of the electronic structure of the interfacial layer should take into account the charge transfer and the penetration of the wave function into the *c*-Si core and the *a*-SiO<sub>2</sub> regions.
- <sup>16</sup>T. Ogawa, K. Shiraishi, K. Takeda, and Y. Kanemitsu (unpublished).
- <sup>17</sup>K. Takeda and K. Shiraishi, *Phys. Rev. B* **39**, 11 028 (1989).
- <sup>18</sup>M. Shinada and S. Sugano, *J. Phys. Soc. Jpn.* **21**, 1936 (1966).
- <sup>19</sup>The calculation of exciton properties takes into account the dielectric effect arising from the different dielectric constants of the interfacial region, the *a*-SiO<sub>2</sub> layer, and the *c*-Si core [see M. Kumagai and T. Takagahara, *Phys. Rev. B* **40**, 12 359 (1989)]. A correction due to spherical curvature is also incorporated but is minor for the size of our samples [see Y. Kayanuma and N. Saito, *Solid State Commun.* **84**, 771 (1992)].

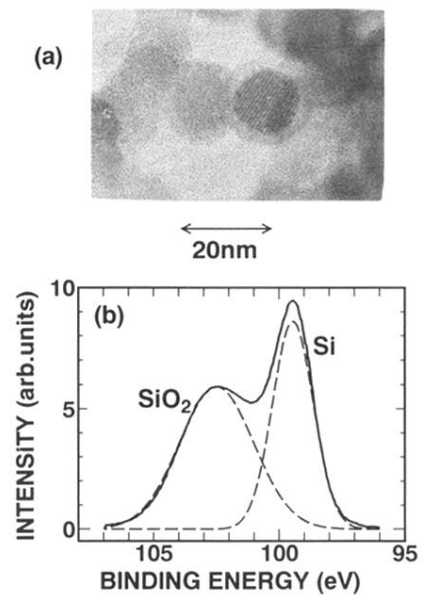


FIG. 1. (a) High-resolution TEM lattice image of oxidized Si nanometer-sized spheres composed of a *c*-Si core and an  $\sim 1.6$ -nm-thick *a*-SiO<sub>2</sub> surface layer. (b) XPS spectrum of the silicon 2*p* region from the oxidized Si nanometer-sized spheres.